DOI: 10.6060/mhc224316z

The First Ate Complex of Copper(II) 5-Chlorosalicylhydroximate Metallacrown with Outer-Sphere Nickel(II) Cation

Galina S. Zabrodina,[@] Marina A. Katkova, Roman V. Rumyantcev, Grigory Yu. Zhigulin, and Sergey Yu. Ketkov

G.A. Razuvaev Institute of Organometallic Chemistry of RAS, 603905 Nizhny Novgorod, Russia
[@]Corresponding author E-mail: kudgs@mail.ru

Recently, there has been a significant interest towards heterometallic 3d-3d metallacrowns (MC) based on salicylhydroxamic acid. In this work, with use of the 5-clorosalicylhydroxamic acid in reaction with the copper(II) and nickel(II) salts the first 12-MC-4 ate complexes bearing the copper(II) ions in the MC ring and an outer-sphere nickel(II) cation were synthesized and characterized. The molecular and crystal structures of complexes were determined from single-crystal X-ray diffraction studies. Detailed DFT studies were carried out for the [Cu(II)[12-MC$_{Cu(II)N(Cl\text{-}shi)}$-4]]$^{2-}$ metallamacrocyclic fragment. The nickel(II) cations appear to promote the formation of a fused metallacrown structure with practically flat copper(II) metallamacrocycles.

Keywords: Metallacrown, 5-chlorosalicylhydroxamic acid, copper(II), nickel(II), ate complex, X-ray structure, DFT.

Первый ат-комплекс медного(II) 5-хлоросалицилгидроксиматного металлакрауна с внешнесферным катионом никеля(II)

Г. С. Забродина,[@] М. А. Каткова, Р. В. Румянцев, Г. Ю. Жигулин, С. Ю. Кетков

Институт металлоорганической химии им. Г.А. Разуваева РАН, 603950 Нижний Новгород, Россия
[@]E-mail: kudgs@mail.ru

В настоящее время наблюдается значительный интерес к гетерометаллическим 3d-3d металлакраунам (MC) на основе салицилгидроксамовой кислоты. С использованием 5-хлорсалицилгидроксамовой кислоты в реакции с солями меди(II) и никеля(II) синтезированы и охарактеризованы первые 12-MC-4 ат-комплексы с ионами меди(II) в кольце MC и внешнесферным катионом никеля(II). Молекулярная и кристаллическая структуры комплексов установлены методом рентгеноструктурного анализа монокристаллов. Детальные исследования методом DFT были проведены для металламакроциклического фрагмента [Cu(II)[12-MC$_{Cu(II)N(Cl\text{-}shi)}$-4]]$^{2-}$. Катионы никеля(II), по-видимому, способствуют образованию сшитой металлакраун-структуры с практически плоскими металламакроциклами меди(II).

Ключевые слова: Металлакраун, 5-хлорсалициловая кислота, медь(II), никель(II), ат-комплекс, РСА, DFT.

Introduction

Metallacrowns (MC) are a unique class of polynuclear metallamacrocyclic complexes forming repeating [M-N-O] subunits with a large variety of fascinating structures of different sizes and topologies.[1-7] Since the first description of these complexes in 1989,[8] salicylhydroxamic acid (H_3shi) has been one of the oldest and frequently used ligands in such systems because of its strong coordination ability toward 3d metal ions, such as V, Cr, Mn, Fe, Co, Ni, Cu and Zn.[9] As a rule the structure of these metallacrowns consists of 3d metal ions located in metallamacrocyclic ring and the same or different metal ion trapped in the central cavity produced by the deprotonated salicylhydroximate ligands. According to the Cambridge Structural Database, most of them represent homo- and heterometallic polynuclear metallamacrocyclic systems based on salicylhydroxamic or substituted salicylhydroxamic acid. This extended salicylhydroximate family of metallacrowns has led to a diversity of the metal-rich structures with homometallic (V(V),[10,11] Cr(III),[12] Mn(II)/Mn(III),[13-17] Fe(III),[18]

Co(II)/Co(III),[9] Ni(II),[19,20] Cu(II),[21-23] and Zn(II)[24]) or heterometallic (Ni(II)/Mn(III),[20,25] Cu(II)/Fe(III),[23] Mn(III)/Cu(II)[26,27]) compositions.

Note, that while the first metallacrowns tended to be homometallic, recently heterometallic complexes have become more in demand. Accordingly, the selection of suitable metal ions is very important. Whereas, despite these well-characterized examples of heterometallic 3d-3d metallacrowns, a strategy to obtain Cu(II)/Ni(II) assemblies using the metallacrown analogy has not been developed. Herein we report the synthetic scheme and structural descriptions of the first example of copper(II) metallacrown ate complexes with outer-sphere nickel(II) cations.

Experimental

General Procedures

All chemicals were reagent-grade and were used as received from Sigma Aldrich without any additional purification. The 5-chlorosalicylhydroxamic acid was synthesized via 5-chlorosalicylic acid according to the literature method[28]. The C, H, N elemental analyses were performed by the Microanalytical laboratory of IOMC RAS on Euro EA 3000 Elemental Analyser. IR spectra were obtained on a Perkin Elmer 577 spectrometer and recorded from 4000 to 450 cm^{-1} as a Nujol mull on KBr plates.

*Synthesis of complexes **1** and **2**.* 5-Chlorosalicylhydroxamic acid (Cl-shiH_3; 0.19 g, 1 mmol) was dissolved in MeOH:DMF (2:1) and mixed with solution of copper(II) acetate dihydrate (0.25g, 1.25 mmol) and nickel(II) chloride hexahydrate (0.48 g, 2 mmol). The emerald dark-green solution was obtained and after one hour, the formation of a precipitate was observed. The reaction mixture was left to stir overnight and after that, the solution and precipitate were separated by filtration and collected. The isolation of complexes was carried out as follows:

*$[Ni(DMSO)_6]^{2+}[Cu(II)[12\text{-}MC_{Cu(II)N(Cl\text{-}shi)}\text{-}4]]^{2-}(DMSO)(H_2O)_{0.5}$ **(1)**.* The green-grey solid residue was washed with methanol and recrystallized from DMSO. Slow evaporation of solvent resulted in the dark-green plate-shaped crystals of **1** suitable for X-ray structure determination after one month. Found: C 30.27, H 3.29, N 3.31%. $C_{84}H_{110}Cl_8Cu_{10}N_8Ni_2O_{39}S_{14}$ requires C 30.20, H 3.32, N 3.35. IR (KBr) ν cm^{-1}: 1595m (ν(C= N)), 1565s (ν(CN)/ν(CO)), 1518m (δ(C-H)), 1412s (δ(C-H)), 1307s, 1245s (ν(N–O)), 1110s, 1022m , 1008s (ν(S-O)DMSO), 820s, 691m, 630m, 541m, 477m.

*$[Ni(DMF)_3(H_2O)_3]^{2+}[Cu(II)[12\text{-}MC_{Cu(II)N(Cl\text{-}shi)}\text{-}4]]^{2-}(DMF)_2(H_2O)_2$ **(2)**.* The dark-green clear filtrate was left for slow evaporation at room temperature. Dark-green plate-shaped crystals of **2** suitable for X-ray structure determination were collected after two weeks. Found: C 32.87, H 3.64, N 8.00%. $C_{86}H_{114}Cl_8Cu_{10}N_{18}Ni_2O_{44}$ requires C 32.89, H 3.66, N 8.03. IR (KBr) ν cm^{-1}: 1648s (ν(C=O)$_{DMF}$), 1598m (ν(C= N)$_{Cl\text{-}shi}$), 1562s (ν(CN)/ν(CO)), 1521m (δ(C-H)), 1416s (δ(C-H)), 1308s, 1244s (ν(N–O)), 1112s, 1023m, 822s, 692m, 631m, 543m, 477m.

X-Ray Crystallographic Studies

The X-ray diffraction data for complexes **1** and **2** were collected on a Bruker D8 Quest diffractometer (Mo-K_α radiation, ω-scan technique, λ = 0.71073 Å). The intensity data were integrated by SAINT program.[29] SADABS program[30] was used to perform absorption corrections. The both structures were solved by dual method[31] and refined on F_{hkl}^2 using SHELXTL package.[32] All non-hydrogen atoms were refined anisotropically. The water hydrogen atoms in **1** and **2** were located from the differential Fourier map and were refined isotropically with thermal ($U_{iso}(H) = 1.2U_{eq}(O)$) and geometry (DFIX) constraints. All other hydrogen atoms were placed in calculated positions and were refined in the riding model ($U_{iso}(H) = 1.5U_{eq}(C)$ for CH_3-groups and $U_{iso}(H) = 1.2U_{eq}(C)$ for other groups). The asymmetric unit of **1** contains a solvate water molecule per two metallamacrocycles. In its turn, there are four DMF and two water molecules per two metallamacrocycles of complex **2**. Structural model of complexes **1** and **2** include massive disorders in the coordination sphere of nickel cation. All coordinated DMSO molecules in complex **1** are disordered over two positions. Also, two coordinated and two solvate DMF molecules in **2** are disordered over two positions. The disordered fragment in complexes **1** and **2** was modelled and refined with restraints of geometry (DFIX and FLAT) and thermal parameters (EADP, RIGU and ISOR).

The crystal data for **1** ($C_{84}H_{110}Cl_8Cu_{10}N_8Ni_2O_{39}S_{14}$): monoclinic crystal system, space group $P2_{1/n}$, unit cell dimensions: a = 18.3100(12) Å, b = 19.0439(13) Å, c = 18.9007(12) Å, β = 112.079(2), V = 6107.3(7) $Å^3$, Z = 2, $d_{calc.}$ = 1.817 Mgm^{-3}, μ = 2.498 mm^{-1}, F(000) = 3376, Crystal size 0.39×0.33×0.28 mm^3, 2.233<θº<27.483, reflections collected/unique = 86965/13984, R_{int} = 0.0517, R_1 = 0.0865, wR^2 = 0.1586 (I > 2s(I)), R_1 = 0.0546, wR^2 = 0.1358 (all data), $S(F^2)$ = 1.012, largest diff. peak and hole 1.865 and -1.158 $eÅ^{-3}$.

The crystal data for **2** ($C_{86}H_{114}Cl_8Cu_{10}N_{18}Ni_2O_{44}$): monoclinic crystal system, space group $P2_{1/n}$, unit cell dimensions: a = 10.6253(4) Å, b = 21.2153(8) Å, c = 24.9986(10) Å, β = 93.0930(10), V = 5626.9(4) $Å^3$, Z = 2, $d_{calc.}$ = 1.853 Mgm^{-3}, μ = 2.460 mm^{-1}, F(000) = 3180, Crystal size 0.20×0.12×0.10 mm^3, 2.146<θº<26.087, reflections collected/unique = 74744/11142, R_{int} = 0.0256, R_1 = 0.0328, wR^2 = 0.0802 (I > 2s(I)), R_1 = 0.0380, wR^2 = 0.0802 (all data), $S(F^2)$ = 1.016, largest diff. peak and hole 1.959 and -0.986 $eÅ^{-3}$.

CCDC 2160669 for **1** and 2160670 for **2** contain the supplementary crystallographic data for this paper. These data can be obtained free of charge from the Cambridge Crystallographic Data Centre via www.ccdc.cam.ac.uk.

Computational Details

Electronic structure of the $\{Cu(II)[12\text{-}MC_{Cu(II)N(Cl\text{-}shi)}\text{-}4]\}^{2-}$ monomeric fragment was investigated employing the density functional theory (DFT). Corresponding quantum chemical calculations were performed with the PRIRODA program suite[33,34] (version 20) which had been shown to treat correctly the hydroximate metallacrowns.[35] The OLYP functional[36] and L2a basis set from the b2n.in basis set array[37] were applied. The OLYP functional is widely used for DFT studies of transition metal complexes.[38] The L2a basis set is an original correlation-consistent all-electron basis set of the triple-ζ polarized quality including diffuse functions (an analogue of well-known aug-cc-pVTZ). The geometries of the $\{Cu(II)[12\text{-}MC_{Cu(II)N(Cl\text{-}shi)}\text{-}4]\}^{2-}$ complex were fully optimized in the high-spin sextet and low-spin doublet states with gradient convergence threshold of 10^{-5} a.u. Further calculations of the harmonic vibrational frequencies testified the structures optimized to be local minima without imaginary eigenvalues. The isosurfaces of the spin density and electron localization function (ELF) were generated with the GABEDIT software[39] (version 2.5.0).

Results and Discussion

The utilization of 5-clorosalicylhydroxamic acid in reaction with the copper(II) and nickel(II) salts results in the formation of a new metallacrown-based ate-complex (Scheme 1).

The further isolation from DMSO and DMF lead to formation of complexes **1** and **2**, respectively. Both complexes are stable in air, insoluble in water, chloroform, acetone, slightly soluble in acetonitrile and methanol, and well soluble in DMSO and DMF. The molecular structures of complexes **1** and **2** were determined by single-crystal X-ray diffraction studies. The asymmetric unit cell of these crys-

tals contains a monomeric fragment of the anionic part and a cationic part of the *ate*-complex (Figures 1, 2). All main bond lengths in the metallamacrocycle of **1** are in good agreement with complex **2** (Table 1) and previously published related compounds.[21,23]

The central copper cation additionally coordinates one DMSO molecule. In the crystal, the neighboring metallacrown molecules are arranged in such a way that the intermolecular Cu(3)–O(6) distance is 2.699(4) Å. This value is typical for the coordination bond O→Cu.[40] Therefore, the anionic fragment of *ate*-complex **1** is a dimer, the monomeric fragments of which are connected to each other through two coordination Cu-O interactions (Figure 3).

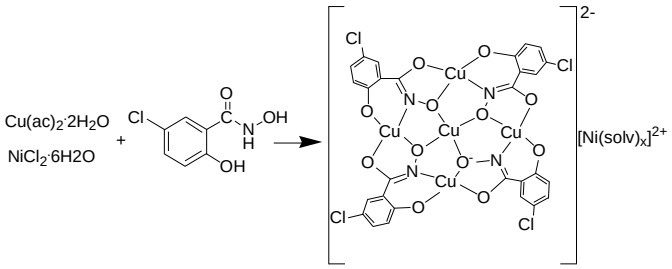

Scheme 1. Synthetic pathway to Cu(II)-Ni(II) metallacrown-based ate-complex.

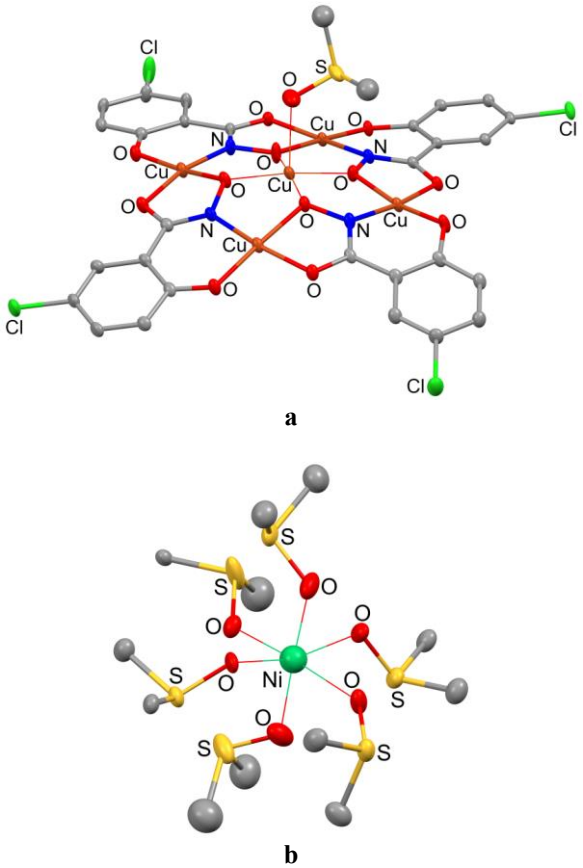

Figure 1. Monomeric fragment of the anionic part (**a**) and cationic part (**b**) of the *ate*-complex **1**. The thermal ellipsoids are drawn at the 30% probability level. All hydrogen atoms are omitted for clarity.

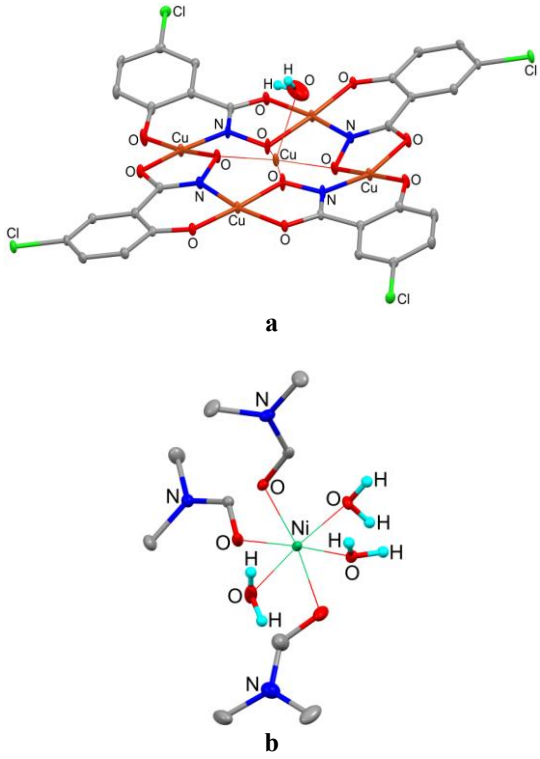

Figure 2. Monomeric fragment of the anionic part (a) and cationic part (b) of the ate-complex 2. The thermal ellipsoids are drawn at the 30 % probability level. Only selected hydrogen atoms are shown in the figure for clarity.

The distance between the center of the phenyl ring of one metallacrown molecule and the central copper atom of the second metallacrown (3.553 Å) suggests the presence of a cation…π interaction between the metallamacrocycles in the dimer. This distance is close to van der Waals contact that is classifiable as the electrostatic interaction.[41] Consequently, the formal coordination number for the central copper atom increases to six, and the coordination environment is a distorted octahedron. The nickel atom in the cationic part of the complex is coordinated by six neutral DMSO molecules (Figure 1b). The coordination environment of the Ni cation is also a distorted octahedron.

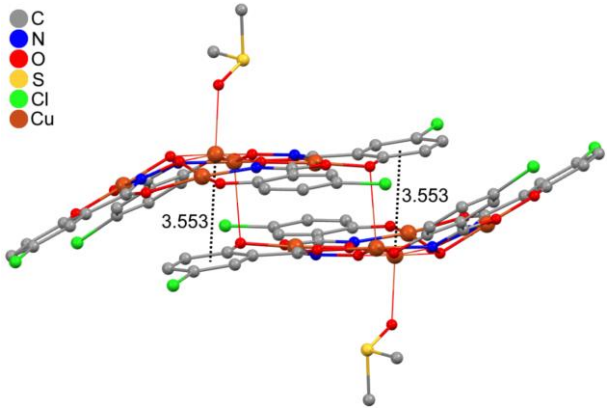

Figure 3. Dimeric structure of the anionic part of complex **1**. All hydrogen atoms are omitted for clarity.

Table 1. The selected bond lengths (Å) and angles (°) in the compounds **1** и **2**.

Distances [Å] and angles [°]	**1**	**2**
Cu(1)-O(oxime)	1.890(3)-1.927(3)	1.885(2) - 1.9413(19)
Cu(1)-O(Solv)	2.290(6)	2.344(4)
Cu-O(oxime)	1.879(4) - 1.915(3)	1.876(2) - 1.9282(19)
Cu-O(carbonyl)	1.936(3) - 1.966(3)	1.9632(19)- 1.9894(18)
Cu-O(phenolate)	1.881(3) - 1.896(3)	1.8735(19) - 1.900(2)
Cu-N(imine)	1.910(4) - 1.944(4)	1.926(2) -1.944(2)
Cu(crown)-O(crownA*)	2.699(4)	2.467(2), 2.713(3), 2.781(2)
C-Cl	1.736(5) - 1.747(5)	1.747(3) - 1.752(3)
Ni(1)-O(Solv)	2.068(6) - 2.155(14)	2.025(2) - 2.099(7)
O(oxime)-Cu-N(imine)	88.44(15) - 91.23(15)	88.85(9) - 92.70(9)
O(oxime)-Cu-O(carbonyl)	80.63(14) - 81.11(14)	80.15(8) - 81.42(8)
O(phenolate)-Cu-N(imine)	91.17(16) - 92.59(16)	90.03(9) - 93.26(9)
O(oxime)-Cu(1)-O(oxime)	87.78(15) -90.78(14); 169.86(19), 172.66(17)	86.75(8) -93.25(8); 171.48(10), 174.70(9)
O(Solv)-Ni(1)-O(Solv)	76.1(4) - 104.1(3); 163.6(2)-177.3(3)	85.11(11) - 96.43(10); 171.3(2) -175.05(10)

*Symmetry transformations used to generate equivalent atoms (A): –x+1, –y, –z+1 for complex **1** and –x+1, –y+1, –z+1 for complex **2**.

The metallamacrocycles in complex **1** are largely non-planar. A bend passing through three copper atoms is observed. The dihedral angle between two planes built through the halves of the molecule separated by copper atoms is 29.32°.

The intermolecular O…H distances in crystal **1** significantly exceed the value characteristic of the contracted contacts (> 2.15 Å).[42] A fragment of the crystal packing of complex **1** is shown in Figure 4.

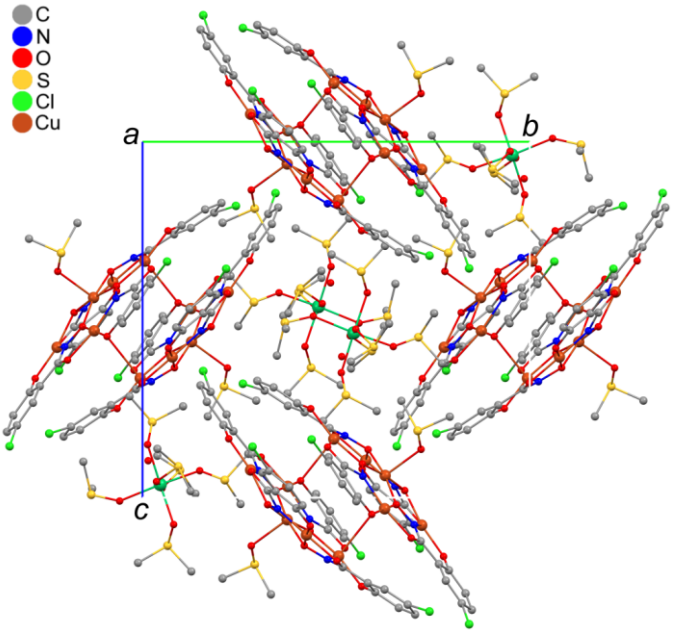

Figure 4. Fragment of crystal packing of complex **1**. The projection along the crystallographic *a* axis.

The asymmetric unit cell of crystal **2** also contains the monomeric fragment of the anionic part and the cationic part of the *ate*-complex (Figure 2). In contrast to complex **1**, the central copper cation in complex **2** coordinates the oxygen of the water molecule. Despite the fact that the anionic fragment of complex **2** is also a dimer of metallacrowns bound via Cu–O coordination bonds, their structure differs significantly (Figure 5). Two practically flat metallacrowns are arranged in a face-to-face orientation relative to each other with only a slight offset. As a result, six Cu-O interactions are observed between two metallamacrocycles in complex **2**. Distances vary in the wide range 2.467(2) – 2.781(2) Å (Table 1). In addition, the distances between the centers of the phenyl rings of two metallacrowns are 3.693 and 3.769 Å, which indicates the presence of weak π…π interactions between them[43].

Thus, as in the case of complex **1**, the coordination environment of the central Cu atom in complex **2** is a distorted octahedron, and the coordination number is equal to six. In both complexes, the central copper atom of the metallamacrocycle slightly deviates from the plane formed by four oxygen atoms of crown (0.143 and 0.112 Å in complexes **1** and **2**, respectively).

The nickel cation in **2**, in contrast to complex **1**, is coordinated by three water molecules and three DMF molecules (Figure 2b). It should be noted that the crystal structure of the related ate complex of copper and manganese, in which two water molecules and four DMF molecules are coordinated on Mn^{2+},[27] differs significantly from complex **2**. Two anionic metallamacrocycles in this complex are located in such a way that the presence of intermolecular Cu-O bonds between these metallacrowns is completely excluded. This fact additionally indicates the important role of neutral solvent molecules in the formation of the crystal structure of such complexes.

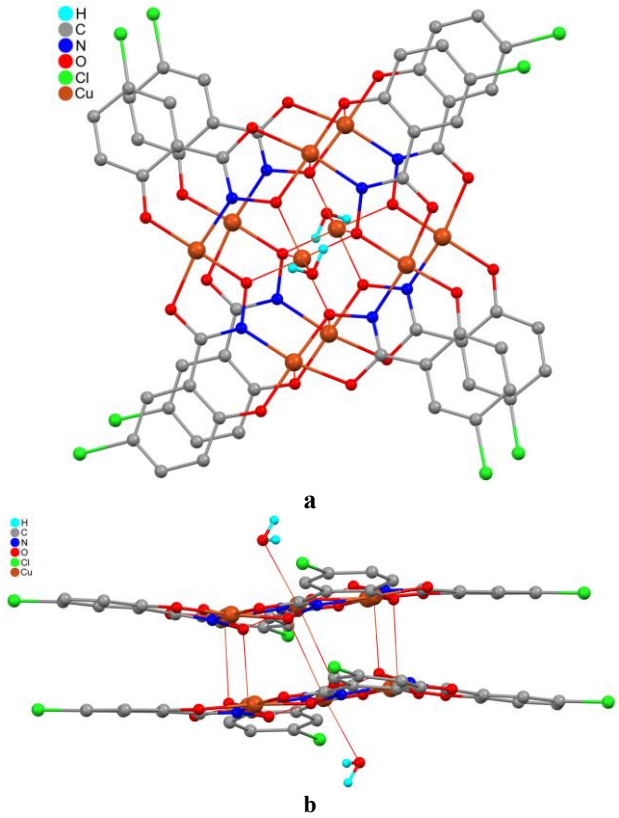

Figure 5. Dimeric structure of the anionic part of complex **2**. Projections along the crystallographic *a* (**a**) and *c* (**b**) axes.

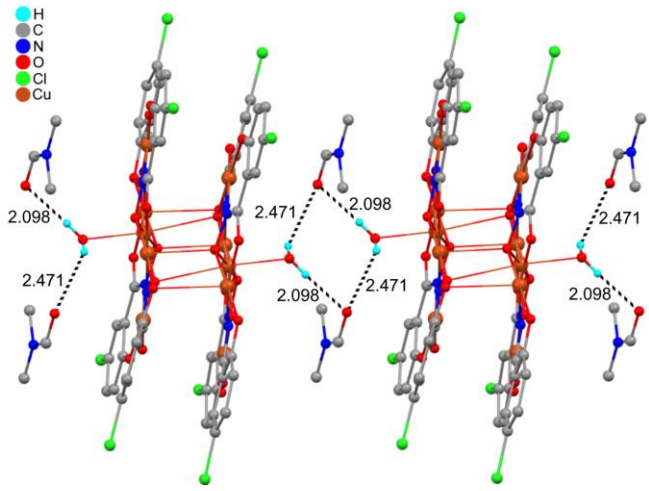

Figure 6. Fragment of an infinite chain formed by anionic fragments of complex **2** and uncoordinated DMF molecules.

In the crystal of complex **2**, two main structural motifs can be identified. Anionic fragments of the complex due to intermolecular O-H…O interactions with free DMF molecules form endless chains (Figure 6). The distances between hydrogen and oxygen atoms H…O are 2.098 and 2.471 Å. Thus, the first interaction can be attributed to the contracted intermolecular contacts (< 2.15 Å).[42] In turn, the distance of 2.471 Å only slightly exceeds the mean length of the normal van der Waals contact for these atoms (2.45 Å).[42]

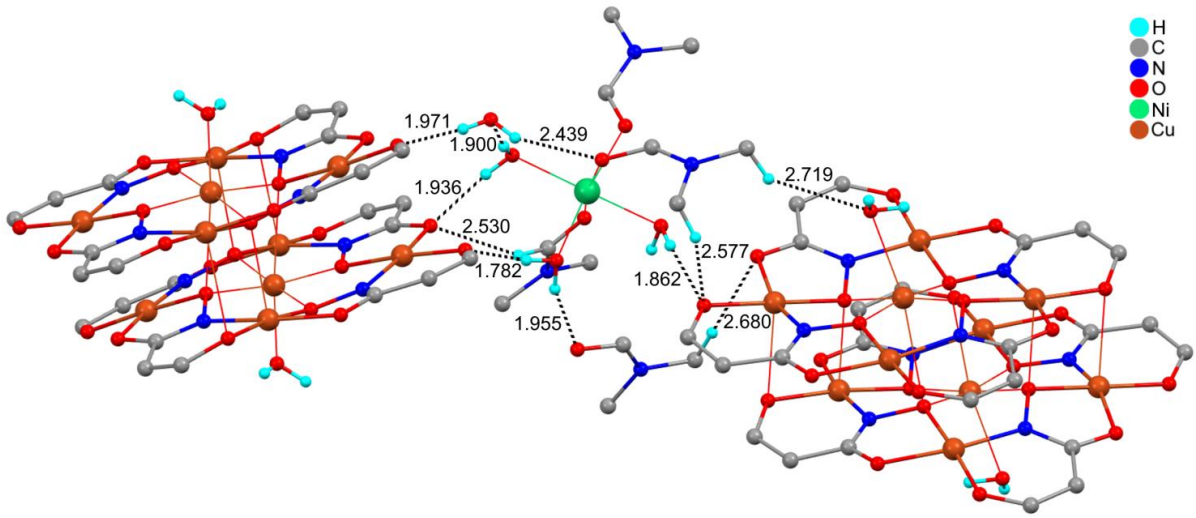

Figure 7. Fragment of the crystal packing of complex **2**. Phenyl groups of metallacrowns and some hydrogen atoms are omitted for clarity.

Infinite chains consisting of anionic fragments of *ate*-complex and DMSO molecules in crystal **2** are connected to each other through cationic fragments, as well as solvate molecules of water and DMSO (see Figure 7). In total, the 11 intermolecular O…H interactions can be distinguished, six of which are contracted contacts (1.782 – 1.971 Å). All other O…H interactions vary in the range of 2.439 – 2.719 Å, which is close to the mean length of the normal van der Waals contact (2.45 Å).[42]

Therefore, the network of intermolecular O…H interactions in crystal **2** is formed due to water hydrogen atoms. It is important to note that both metallacrowns in the dimeric anionic fragment of the *ate*-complex are directly involved in the formation of these contacts. Replacing the solvent with DMSO leads to the destruction of intermolecular O…H interactions and, as a consequence, the formation of a new configuration of the anionic part of the complex.

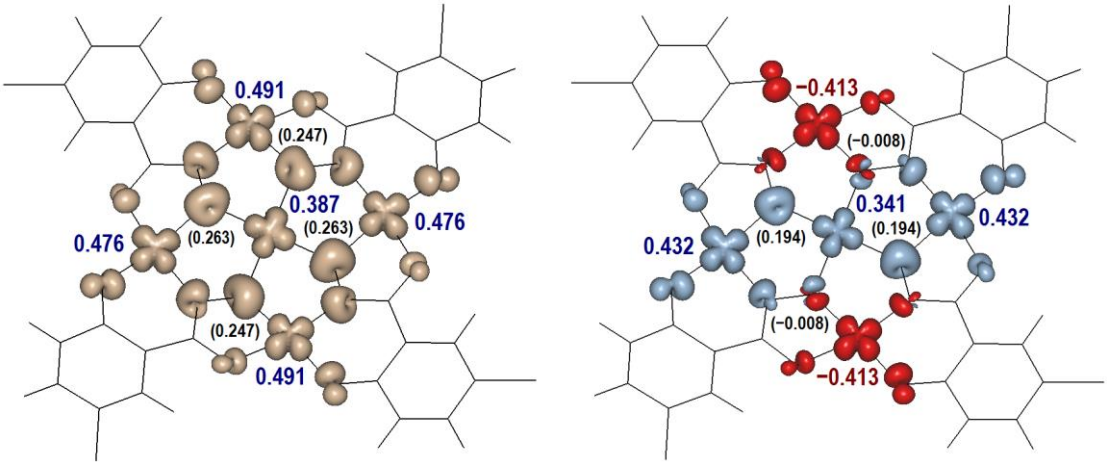

Figure 8. Spin density isosurfaces (0.01 a.u.) for the sextet (left) and doublet (right) states of the $\{Cu(II)[12\text{-}MC_{Cu(II)N(Cl\text{-}shi)}\text{-}4]\}^{2-}$ complex with the Mulliken spin populations for the copper and oxime oxygen atoms (in parentheses). The DFT level is OLYP/L2a.

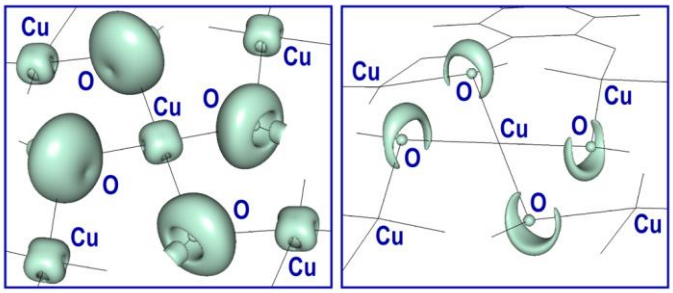

Figure 9. ELF isosurfaces at η(r) = 0.750 (left) and η(r) = 0.885 (right) for the copper and oxime oxygen atoms in the high-spin sextet state of the $\{Cu(II)[12\text{-}MC_{Cu(II)N(Cl\text{-}shi)}\text{-}4]\}^{2-}$ complex.

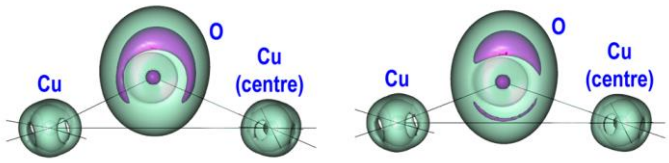

Figure 10. Comparison of the ELF topologies for the CuOCu site in the sextet (left) and doublet (right) spin states of the $\{Cu(II)[12\text{-}MC_{Cu(II)N(Cl\text{-}shi)}\text{-}4]\}^{2-}$ complex: combinations of the ELF isosurfaces at η(r) = 0.750 (green translucent) and η(r) = 0.885 (pink opaque).

Electronic structure of the $\{Cu(II)[12\text{-}MC_{Cu(II)N(Cl\text{-}shi)}\text{-}4]\}^{2-}$ metallamacrocyclic fragment was investigated using the DFT calculations. For the $\{Cu(II)[12\text{-}MC_{Cu(II)N(Cl\text{-}shi)}\text{-}4]\}^{2-}$ monomeric dianionic complex the high-spin sextet and low-spin doublet states were simulated at the OLYP/L2a level of DFT (Figure 8). The optimized structural parameters are close to those obtained by the X-ray crystallographic experiment (Table 1). In particular, for the sextet/doublet states calculated Cu(1)-O(oxime) distances are 1.990–1.998/1.953–1.979 Å and Cu-N(imine) bonds are 1.948–1.957/1.942–1.967 Å. Accumulation of the copper spin density is oriented toward the O and N atoms in both the sextet and doublet states. Such localization of the spin density at the Cu(II) ions corresponds to the $3d_{x^2-y^2}$ orbital which is formally single occupied. The central Cu(II) ion in both sextet and doublet is characterized by the lower absolute value of spin population than the peripheral cations. For the low-spin doublet state our DFT calculations predict alternation of the negative (–0.413) and positive (0.432) spin populations among the peripheral Cu(II) ions, the central ion bearing the positive value of 0.341. Notably, two of four bridging oxime oxygen atoms in the low-spin complex are described by the values of –0.008 close to zero. Such spin populations arise due to the antiferromagnetic exchange between the Cu(II) ions. Moreover, computed values of the electron energy, $H°(298.15)$, and $G°(298.15)$ decrease on going from the sextet to doublet by 5.4, 5.9, and 4.6 kcal/mol, respectively. Thus, the antiferromagnetic exchange between the Cu(II) ions stabilizes the low-spin doublet state of the $\{Cu(II)[12\text{-}MC_{Cu(II)N(Cl\text{-}shi)}\text{-}4]\}^{2-}$ complex.

Another quantum chemical approach efficiently used for description of the hydroximate metallacrowns is electron localization function (ELF), η(r).[44-46] Based on local increase of the kinetic energy density associated with the Pauli Exclusion Principle the function reveals localization attractors corresponding to the core, bonding and non-bonding electron pairs and defines their topology.[47,48] The η(r) values of ELF change from 0 to 1: at η(r) → 1 the electron pairs are localized; at η(r) = 1/2 full delocalization of electrons realizes (that corresponds to the electron gas); at η(r) → 0 separation of the electron pairs occurs. The ELF isosurface calculated at η(r) = 0.750 for the $\{Cu(II)[12\text{-}MC_{Cu(II)N(Cl\text{-}shi)}\text{-}4]\}^{2-}$ complex (Figure 9) detects domains of lone pairs for the bridging oxime oxygen atoms and contributions of core 3*d* electrons for the Cu(II) ions. The ELF topology round the copper nuclei is not spherically symmetric: four holes oriented along the coordination bonds are clearly seen. These holes appear due to lower (formally single) occupancy of $3d_{x^2-y^2}$ in comparison with double occupancy of the other 3*d* orbitals. For the bridging oxime oxygen atoms increase of the η(r) value to 0.885 reveals remarkable electron localization outside the CuOCu planes

(Figures 9, 10) that is explained by excess of the negative charge on the $\{Cu(II)[12\text{-}MC_{Cu(II)N(Cl\text{-}shi)}\text{-}4]\}^{2-}$ complex. Variation of the multiplicity changes slightly the ELF topology round the oxime oxygen nuclei but the significant electron localization outside the CuOCu planes remains unchanged (Figure 10). Thus, accumulation of the electron density in the apical positions of the oxime oxygen atoms promotes formation of the Cu–O(oxime) intermolecular interactions in the crystal structure of the dimeric complex.

Conclusions

In summary, we have attempted to highlight some novel synthetic and structural aspects of chemistry of the 3d-3d metallacrowns bearing salicylhydroximate ligands. The use of 5-ClshiH_3 in reaction with copper(II) and nickel(II) salts results in the formation of a new family of ate complexes with the copper(II) ions in the MC ring. The compounds obtained contain two offset stacked anionic units and outer-sphere nickel(II) cations. Thus, the nickel(II) cations promote formation of a fused metallacrown structure with face-to-face orientation relative to the practically flat copper(II) metallamacrocycles.

Acknowledgements. This research was funded by the Russian Science Foundation (project No. 18-13-00356). The work was carried out using the equipment of the center for collective use "Analytical Center of the IOMC RAS" with the financial support of the grant "Ensuring the development of the material and technical infrastructure of the centers for collective use of scientific equipment" (Unique identifier RF----2296.61321X0017, Agreement Number 075-15-2021-670).

References

1. Lah M.S., Pecoraro V.L. *Comments Inorg. Chem.* **1990**, *11*, 59–84. https://doi.org/10.1080/02603599008035819.
2. Bodwin J.J., Cutland A.D., Malkani R.G., Pecoraro V.L. *Coord. Chem. Rev.* **2001**, *216–217*, 489–512. https://doi.org/10.1016/S0010-8545(00)00396-9.
3. Mezei G., Zaleski C.M., Pecoraro V.L. *Chem. Rev.* **2007**, *107*, 4933–5003. https://doi.org/10.1021/cr078200h.
4. Tegoni M., Remelli M. *Coord. Chem. Rev.* **2012**, *256*, 289–315. https://doi.org/10.1016/j.ccr.2011.06.007.
5. Ostrowska M., Fritsky I.O., Gumienna-Kontecka E., Pavlishchuk A.V. *Coord. Chem. Rev.* **2016**, *327–328*, 304–332. https://doi.org/10.1016/j.ccr.2016.04.017.
6. Pavlyukh Y., Rentschler E., Elmers H.J., Hubner W., Lefkidis G. *Phys. Rev.* **2018**, *B97*, 214408. https://doi.org/10.1103/ PhysRevB.97.214408.
7. Katkova M.A. *Russ. J. Coord. Chem*. **2018**, *44*, 284–300. https://doi.org/10.1134/S107032841804005X.
8. Lah M.S., Pecoraro V.L. *J. Am. Chem. Soc.* **1989**, *111*, 7258–7259. https://doi.org/10.1021/ja00200a054.
9. Happ P., Plenk Ch., Rentschler E. *Coord. Chem. Rev*. **2015**, *289-290*, 238–260. https://doi.org/10.1016/j.ccr.2014.11.012
10. Si T.K., Chakraborty S., Mukherjee A.K., Drew M.G.B., Bhattacharyya R. *Polyhedron* **2008**, *27*, 2233–2242. https://doi.org/10.1016/j.poly.2008.03.031.
11. Pecoraro V.L. *Inorg. Chim. Acta* **1989**, *155*, 171–173. https://doi.org/10.1016/S0020-1693(00)90405-5.
12. Lupke A., Carrella L.M., Rentschler E. *Chem.-Eur. J.* **2021**, *27*, 4283–4286. https://doi.org/10.1002/chem.202004947.
13. Tigyer B.R., Zeller M., Zaleski C.M. *Acta Cryst.* **2011**, *E67*, m1041–m1042. https://doi.org/10.1107/S160053681102602X.
14. Tigyer B.R., Zeller M., Zaleski C.M. *Acta Cryst.* **2012**, *E*68, m1521–m1522 https://doi.org/10.1107/S1600536812047228.
15. Tigyer B.R., Zeller M., Zaleski C.M. *Acta Cryst.* **2013**, *E*69, m393–m394. https://doi.org/10.1107/S1600536813015857.
16. Lutter, J.C., Kampf, J.W., Zeller M., Zaleski C.M. *Acta Cryst.* **2013**, *E*69, m483–m484. https://doi.org/10.1107/S1600536813021314.
17. Zaleski C.M., Lutter, J.C., Zeller M. *J. Chem. Crystallogr*. **2015**, *45*, 142–150. https://doi.org/10.1007/s10870-015-0576-0.
18. Chow C.Y., Guillot R., Riviere E., Kampf J.W., Mallah T., Pecoraro V.L. *Inorg. Chem.* **2016**, *55*, 10238–10247. https://doi.org/10.1021/acs.inorgchem.6b01404.
19. Psomas G., Dendrinou-Samara C., Alexiou M., Tsohos A., Raptopoulou C.P., Terzis A., Kessissoglou D.P. *Inorg. Chem.* **1998**, 37, 6556–6557. https://doi.org/10.1021/ic980614t.
20. Psomas G., Stemmler A.J., Dendrinou-Samara C., Bodwin J.J., Schneider M., Alexiou M., Kampf J.W., Kessissoglou D.P., Pecoraro V.L. *Inorg. Chem.* **2001**, *40*, 1562–570. https://doi.org/10.1021/ic000578.
21. Plenk C., Krause J., Beck M., Rentschler E. *Chem. Commun.* **2015**, *51*, 6524–6527. https://doi.org/10.1039/C5CC00595G
22. Herring J., Zeller M., Zaleski C.M. *Acta Cryst*. **2011**, *E67*, m419–m420. https://doi.org/10.1107/S1600536811007975.
23. Happ P., Rentschler E. *Dalton Trans.* **2014**, *43*, 15308–15312. https://doi.org/10.1039/C4DT02275K.
24. Alexiou M., Dendrinou-Samara C., Raptopoulou C.P., Terzis A., Kessissoglou D.P. *Inorg. Chem.* **2002**, *41*, 4732–4738. https://doi.org/10.1021/ic0200904.
25. Hall A.J., Zeller M., Zaleski C.M., *Acta Cryst.* **2020**, *E76*, 1720–1724. https://doi.org/10.1107/S205698902001316X.
26. Lewis A.J., Garlatti E., Cugini F., Solzi M., Zeller M., Carretta S., Zaleski C.M. *Inorg. Chem.* **2020**, *59*, 11894–11900. https://doi.org/10.1021/acs.inorgchem.0c01410.
27. Van Trieste III G.P., Zeller M., Zaleski C.M., *Acta Cryst.* **2020**, *E76*, 747–751. https://doi.org/10.1107/S2056989020005770.
28. Cao F., Wang S., Li D., Zeng S., Niu M., Song Y., Dou J. *Inorg. Chem.* **2013**, *52*, 10747–10755. https://doi.org/10.1021/ic3025952.
29. SAINT, Data Reduction and Correction Program, Bruker AXS, Madison, WI, **2014**.
30 Krause L., Herbst-Irmer R., Sheldrick G.M., Stalke D. *J. Appl. Crystallogr*. **2015**, *48*, 3–10. https://doi.org/10.1107/S1600576714022985.
31. Sheldrick G.M. *Acta Cryst.* **2015**, *A71*, 3–8. https://doi.org/10.1107/S2053273314026370.
32. Sheldrick G.M. *Acta Cryst*. **2015**, *C71*, 3–8. https://doi.org/10.1107/S2053229614024218.
33. Laikov D.N. *Chem. Phys. Lett.* **1997**, *281*, 151–156. https://doi.org/10.1016/S0009-2614(97)01206-2.
34. Laikov, D.N., Ustynyuk, Y.A. *Russ. Chem. Bull.* **2005**, *54*, 820–826. https://doi.org/10.1007/s11172-005-0329-x.
35. Katkova M.A., Zhigulin G.Y., Rumyantcev R.V., Zabrodina G.S., Shayapov V.R., Sokolov M.N., Ketkov S.Y. *Molecules* **2020**, *25*, 4379. https://doi.org/10.3390/molecules25194379
36. Baker J., Pulay P. *J. Chem. Phys.* **2002**, *117*, 1441–1449. https://doi.org/10.1063/1.1485723.
37. Laikov D.N. *Theor. Chem. Acc.* **2019**, *138*, 40. https://doi.org/10.1007/s00214-019-2432-3.

38. Ghosh A. *Chem. Rev*. **2017**, *117*, 3798–3881. https://doi.org/10.1021/acs.chemrev.6b00590.
39. Allouche A.R. *J. Comput. Chem.* **2011**, *32*, 174–182. https://doi.org/10.1002/jcc.21600.
40. Martins N.M.R., Mahmudov K.T., da Silva M.F.C.G., Martins L.M.D.R.S., Pombeiro A.J.L. *New J. Chem.* **2016**, *40*, 10071–10083. https://doi.org/10.1039/C6NJ02161A.
41. Hori A., Arii T. *Cryst. Eng. Comm*, **2007**, *9*, 215–217. https://doi.org/10.1039/B617808A.
42. Zefirov Yu.V., Zorky P.M. *Russ. Chem. Rev.* **1995**, *64*, 415–428. https://doi.org/10.1070/RC1995v064n05ABEH000157.
43. Janiak C. *J. Chem. Soc., Dalton Trans*. **2000**, 3885–3896. https://doi.org/10.1039/B003010O.
44. Katkova M.A., Zabrodina G.S., Zhigulin G.Yu., Baranov E.V., Trigub M.M., Terentiev A.A., Ketkov S.Yu. *Dalton Trans.* **2019**, *48*, 10479–10487. https://doi.org/10.1039/C9DT01368G.
45. Zabrodina G.S., Katkova M.A., Baranov E.V., Zhigulin G.Yu., Ketkov S.Yu. *Macroheterocycles* **2019**, *12*, 300–306. https://doi.org/10.6060/mhc190866z.
46. Katkova M.A., Zabrodina G.S., Zhigulin G.Yu., Rumyantsev R.V., Ketkov S.Yu. *Russ. J. Coord. Chem.* **2019**, *45*, 721–727. https://doi.org/10.1134/S1070328419100014.
47. Becke A.D., Edgecombe K.E. *J. Chem. Phys.* **1990**, *92*, 5397–5403. https://doi.org/10.1063/1.458517.
48. Savin A., Silvi B., Colonna F. *Can. J. Chem.* **1996**, *74*, 1088–1096. https://doi.org/10.1139/v96-122.

Received 01.04.2022
Accepted 22.04.2022